THE POWER OF SINGLE CHANNEL RECORDING AND ANALYSIS:
Its application to ryanodine receptors in lipid bilayers

D.R. Laver

School of Biochemistry and Molecular Biology, The Faculties,
The Australian National University, Canberra, ACT, 0200

Summary

Since the inception of the patch-clamp technique, single channel recording has made an enormous impact on our understanding of ion channel function and its role in membrane transport and cell physiology. However, the impact of single channel recording methods on our understanding of intracellular Ca^{2+} regulation by internal stores is not as broadly recognized. There are several possible reasons for this. First, ion channels in the membranes of intracellular organelles are not directly accessible to patch pipettes, requiring other methods, which are not as widely known as the patch-clamp techniques. Secondly, bulk assays for channel activity have proved very successful in advancing our knowledge of Ca^{2+} handling by intracellular stores. These assays include Ca^{2+} imaging, ryanodine binding assays and measurements of muscle tension and Ca^{2+} release and uptake by vesicles that have been isolated from internal stores. This review describes methods used for single channel recording and analysis, as applied to the calcium release channels in striated muscle, and details some of the unique contributions that single channel recording and analysis have made to our current understanding of the release of Ca^{2+} from the internal stores of muscle. With this in mind, it focuses on three aspects of channel function and shows how single channel investigations have led to an improved understanding of physiological processes in muscle. Finally, it describes some of the latest improvements in membrane technology that will underpin future advances in single channel recording.

Regulation of intracellular [Ca^{2+}] by internal stores in striated muscle

In many cell types the intracellular free calcium ion concentration is altered by the uptake and release of calcium from internal stores such as the endoplasmic reticulum (ER) and sarcoplasmic reticulum (SR). In striated muscle, intracellular calcium concentration, and hence muscle force and cardiac output, is regulated by release of calcium from the SR via ryanodine receptor calcium channels (RyRs) and uptake via the Ca-ATPase. Ca^{2+} fluxes across the SR often take place in the presence of a changing cytoplasmic milieu during episodes of metabolic challenge such as that seen during hypoxia, ischaemia and fatigue. For example, the large changes in the concentration of cytoplasmic anions such as inorganic phosphate, phosphocreatine, and ATP seen during muscle fatigue have profound effects on SR Ca^{2+} handling. In striated muscle the depolarization of the surface membrane and transverse-tubular (T) system by an action potential (the T-system is an invagination of the surface membrane) triggers calcium release from the SR by a process known as excitation-contraction coupling (EC coupling). Dihydropyridine receptors (DHPRs, L-type calcium channels in the T-system) act as voltage-sensors that detect depolarization due to an action potential. Depolarisation induced activation of DHPRs somehow activates RyRs in the apposing SR membrane. In cardiac muscle the influx of Ca^{2+} through DHPRs is believed to activate RyRs (Nabauer *et al.*, 1989) whereas in skeletal muscle DHPRs are mechanically coupled to RyRs (Tanabe *et al.*, 1990) so that Ca^{2+} influx through the DHPRs receptors is not a prerequisite for muscle contraction (Ashley *et al.*, 1991). However, the specific details of EC coupling are not understood, specifically how it is modulated or limited by various cytoplasmic and luminal factors.

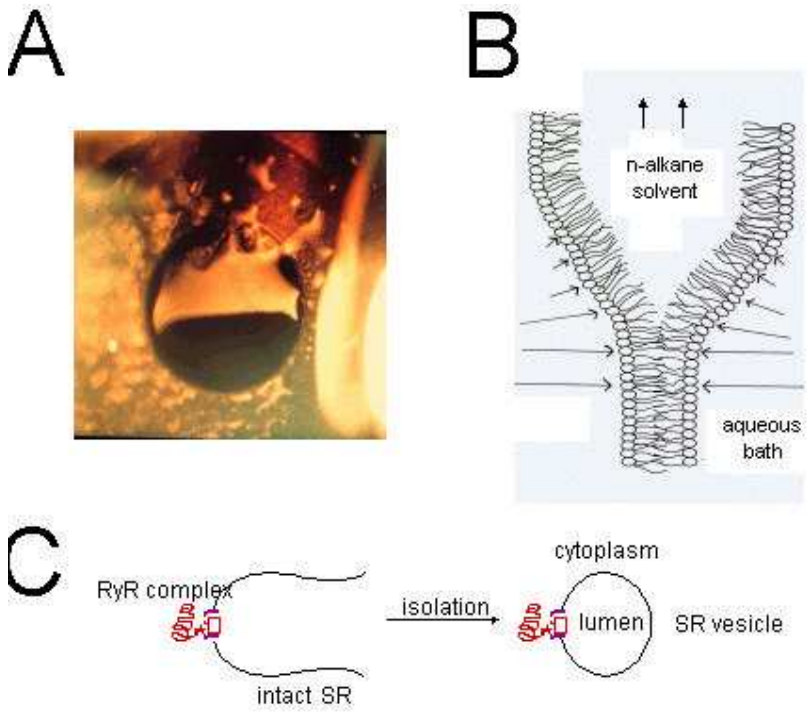

Figure 1. *Formation of lipid bilayers and incorporation of RyRs. (A) A photograph of a lipid bilayer (bottom half of aperture) during its formation from a thick lipid film (top half). The lipid film was spread across an aperture (~100mm diameter) in a delrin septum. The thick lipid film strongly reflects the incident light whereas the bilayer, which shows the black background, is totally transparent. The bilayer portion of the film spreads across the entire aperture in a few seconds leaving a region of thick film at the periphery. (B) A schematic diagram of the process of lipid bilayer formation showing the lipid monolayers that the two oil-water interfaces. The lengths of the arrows, which are shown in each aqueous phase, indicate the relative strengths of the Van der Waals compressive forces between the adjacent water phases. This compressive force squeezes the oil (n-alkane in this case) out from between the monolayers. (C) The procedure for incorporating ion channels form the SR (RyRs in this case) into lipid bilayers. Vesicles of SR membrane (~0.1 mm diameter) are isolated from muscle tissues using differential centrifugation methods. SR vesicle containing ion channels are added to the bath near the lipid bilayer. Fusion of the vesicles with the bilayer carries ion channels into the bilayer membrane.*

The RyR is a homotetramer of ~560 kDa subunits containing ~5035 amino acids. Electron microscope image reconstruction shows RyRs to have four-fold symmetry with a large cytoplasmic domain (the foot region) and a relatively small transmembrane region that forms the Ca^{2+} pore (Orlova *et al.*, 1996). The trans membrane pore is comprised of the ~1000 C-terminal amino acids (aa 4000-5000) and the remaining amino acids form the foot region. In mammals, three isoforms of RyRs have been cloned and sequenced: namely, ryr-1 found in skeletal muscle and brain, ryr-2 most abundantly found in brain and cardiac muscle and ryr-3, though originally found in the brain, is the major isoform in smooth muscle (Ogawa, 1994).

The Bilayer method

At the same time that Neher and Sakmann were developing the patch-clamp technique (Neher and Sakmann, 1976), Miller and Racker (1976) discovered that SR vesicles isolated from muscle could be fused with artificial lipid bilayers and so incorporate ion channels from muscle membranes into artificial membranes. Artificially produced, planar, bimolecular lipid membranes (bilayers) were originally used as model systems for studying cell membrane structure. Their large area (they can be produced with diameters ranging from 1 μm to 1 cm) and planar geometry made them particularly convenient membrane models for electrical and mechanical measurements. For the purposes of studying ion channels, bilayers are usually formed using a modification of the film drainage method developed by (Mueller *et al.*, 1962). A solution of lipids in a hydrophobic solvent (usually n-decane) is smeared across a hole in a plastic septum (eg. Delrin, polycarbonate or Teflon) to produce a thick lipid film separating two baths (Fig. 1A). The bilayer forms spontaneously from this thick lipid film. During bilayer formation the surface-active lipids aggregate into monolayers at the oil-water interfaces on each side of the thick film. The solvent drains away from between the two monolayers thus allowing their apposition and formation of the bilayer structure (Fig. 1B).

Incorporation of ion channels into bilayers is usually simply done by adding ion channel protein to one of the baths and stirring. Ion channel incorporations occur spontaneously and can be detected by conductance changes in the bilayer membrane. For studying the SR ion channels, the bilayers are produced with a diameter of ~100 μm. SR vesicles are added to a final concentration of 1-10 μg/ml and the bath is stirred until channel activity indicates vesicle fusion with the bilayer. The side of the bilayer to which the vesicles are added is usually defined as the *cis* side (Fig. 1C). Conditions that promote vesicle fusion are: 1) a gradient in osmotic potential across the membrane (*cis* high), 2) *cis* $[Ca^{2+}]$ at mM concentrations and 3) vigorous stirring of the *cis* bath. The cytoplasmic side of the SR membrane, when fused with the bilayer, faces the *cis* bath and the luminal side faces the *trans* bath. Stirring of the *cis* and *trans (*cytoplasmic and luminal*)* chambers is usually done using magnetic stirrers.

Cesium methanesulfonate (CsMS) is commonly used as the principal salt in the bathing solutions. This is to prevent current signals from other ion channels from interfering with RyR recordings: the RyR is quite permeable to Cs^+ whereas other ion channels in the SR do not conduct MS^- and Cs^+. Experiments also use a $[Cs^+]$ gradient across the bilayer (250 mM *cis* and 50 mM *trans*) to promote vesicle fusion (see above).

When a vesicle has fused with a bilayer the ion channels embedded in the vesicle membrane become incorporated into the bilayer. Once this happens it is possible to determine the ionic conductance of a single channel and to monitor it's opening and closing (gating) by measuring the current through the membrane in response to an applied electrochemical gradient. The bilayer technique allows considerable flexibility in manipulating the experimental conditions. One can examine the response of channels to a variety of substances in the cytosolic and luminal baths as well as changes in the composition of the bilayer itself. One can also measure channel function under steady-state conditions or when solutions are rapidly and transiently altered. With this experimental technique, like with the patch-clamp technique, it is possible to obtained very detailed information about mechanisms determining channel conductance and gating.

Single channel analysis.

This section is devoted to examining the most commonly used methods for describing the properties of ion channel signals and inferring their mechanisms of function. Single channel signals generally appear as a series of stochastic current jumps between stationary current levels (e.g. see Fig. 2A). For most channel types the jumps are mainly between the closed state and a maximum level (the

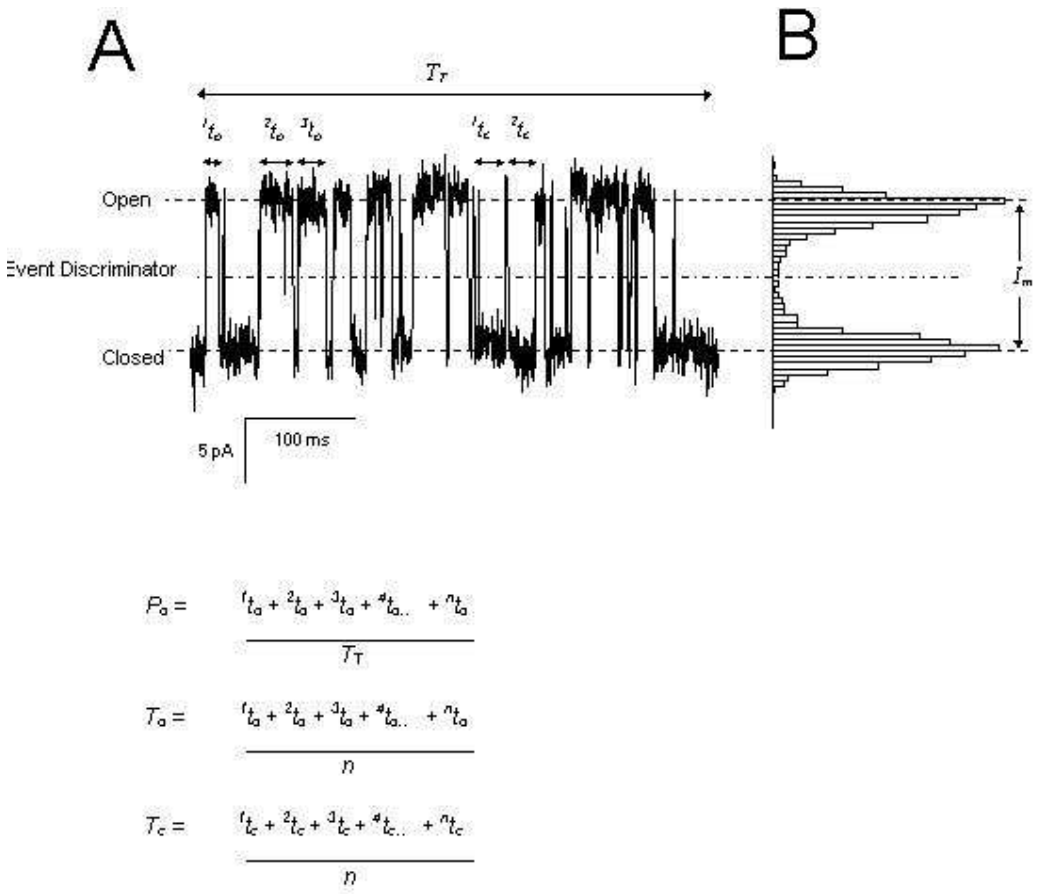

Figure 2. *Analysis of single channel parameters. (A) A typical example of a current signal from a single RyR (left) where channel openings are marked by upward transitions in the current. The dotted lines indicate the current levels corresponding to the open and closed channel. The dashed line shows the current threshold, which defines open and closed events in the analysis. (B) An amplitude histogram of the data in part A which shows a bimodal distribution with peaks corresponding to the stationary current levels (i.e. Open and Closed). The maximum unitary current is I_m. The open and closed dwell times are given by the parameters, ${}^nt_o$ and ${}^nt_c$ respectively. The equations show how open probability, P_o, mean open dwell-time, T_o and mean open dwell-time, T_c, are calculated from the dwell-times.*

unitary current, I_m). Intermediate current levels correspond to subconductance (substates) of the channel.

Channel function is broadly characterised by the amplitudes and durations of stationary current levels. The most popular method for visualizing the different current levels from a channel signal is the all-points amplitude histogram. This is a histogram of all data points grouped according to their amplitude (Fig. 2B). Peaks in the histogram correspond to sustained current levels in the record. The width of the peaks is proportional to the size of the background noise and the area under each peak is proportional to the total time spent at that level. An overall measure of the channel activity can be obtained from the open probability, P_o and the fractional, mean current, *I*. P_o is the fraction of time the channel is in a conducting state and is calculated from the ratio of the number of data points in conducting levels and the total number of points in the record (assuming equally spaced data samples). The fractional, mean current is equal to the time-average of the current amplitude divided by I_m. A value of one indicates that the channel is never closed and a value of zero indicates that the channel is never open. For ion channels with only one open conductance level P_o and *I* give the same value.

Although these parameters provide an overall picture of channel activity, they do not provide much more information than what can be obtained from bulk assays of channel activity.

A more detailed and rewarding analysis of channel activity can be derived from the statistics of amplitudes and durations (i.e. dwell-times: the times spent at each current level before it jumps to a new value). An overall picture of channel gating rates is encapsulated in the mean open and closed dwell-times (T_o and T_c, see Fig. 2). Frequency histograms of open and closed dwell-times graphically show the kinetic signature of the gating mechanism and provide clues to the underlying gating mechanisms (see below). The frequency distributions of dwell-times can be well described by the sum of decaying exponential functions. There are several graphical methods for displaying these histograms, two of which are shown in Figure 3A. The most useful types of plot is that developed by Sigworth and Sine (1987) which is shown in Figure 3B. The data are grouped into bins that are equally spaced on a log scale. In this log-binned scale the broadening of the bins at longer times increases the number of counts in each bin which tends to counter the exponential decline seen in uniformly binned distributions. Distributions that are exponentially distributed on the linear scale form peaked distributions in log-binned histograms where each peak corresponds to an exponential component of the distribution. Probability distributions of dwell-times can be obtained from frequency distributions by dividing the data by the total number of events in the distribution (i.e. the area under the curve becomes one). In addition when the square root of the probability is plotted, the statistical scatter on the data becomes uniform across the entire distribution.

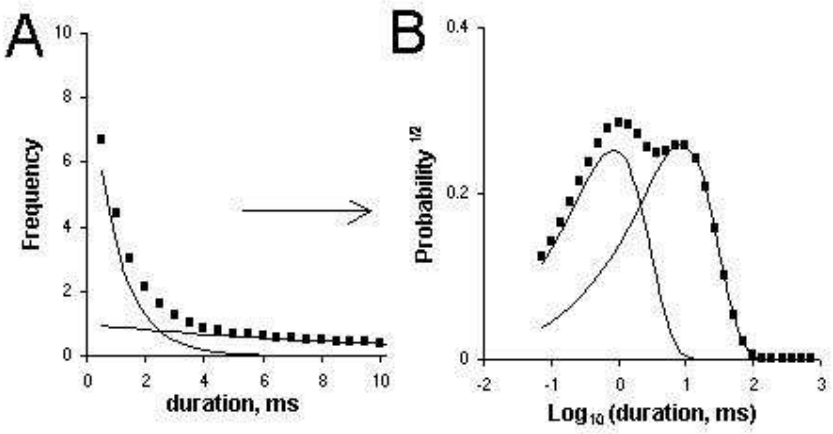

Figure 3. *Frequency histograms of open and closed dwell-times. (A) A fictitious distribution of dwell times, typical of that obtained from single channel recordings, which is comprised of two exponential components with distinctly different decay constants (time constants). (B) The probability distribution from the same dwell-time data is plotted using log-spaced bins (i.e. they appear equally spaced in the log-time scale). The wider bins (in absolute terms) at the right end of the scale tend to collect more data counts than the narrower bins at the left. The probability distribution is calculated by normalizing the frequency distribution according to the area under the curve (see text). Hence the two exponential decays in part A assume a double peaked distribution in part B. The locations of the peaks on the time-scale approximately correspond to the time constants of each exponential.*

From the kinetic signature it is possible to make inferences about the mechanisms underlying the gating processes of the channels. This is illustrated here with a simulated single channel recording based on a six-state gating scheme with three open and three closed states (Fig. 4A). The timing of transitions between states is calculated from the reaction rates using a stochastic algorithm. Figure 4B (circles) shows probability distributions (log-binned) of open and closed dwell-times obtained from the simulated recording. These open and closed probability distributions show three exponential time constants, which are manifest as three peaks in the distributions. Each peak corresponds to a different open or closed state of the reaction scheme. In this simple case, each exponential time constant in Figure

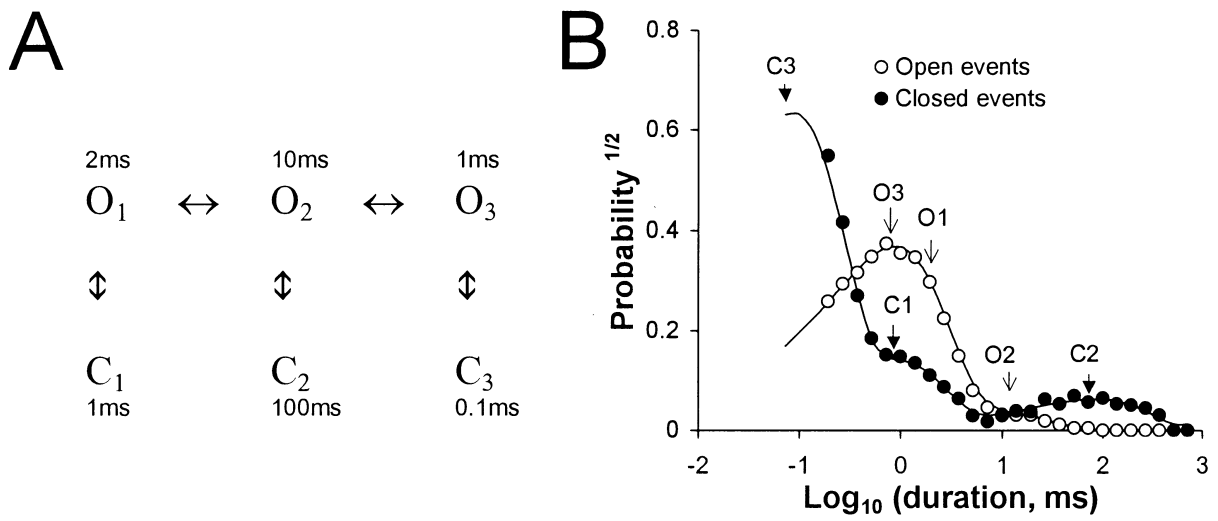

Figure 4. (A) *A reaction scheme describing some of the aspects of RyR gating in which the channel can adopt three different open and closed states. Rather than showing all the reaction rates just the mean lifetimes of each state is shown here. (B) A probability (the square root) distribution of open (○) and closed (●) dwell-times obtained from a simulated, single channel recording which was generated from a gating mechanism given by the Scheme shown in part A (see text). The arrows indicate the peaks in the distributions that correspond to the various states in the gating scheme. The solid lines are theoretical probability functions derived from the gating scheme in part A, using the method of Colquhoun and Hawkes (1981).*

4B (arrows) corresponds approximately in value to the average time spent in each state in Figure 4A. Generally, the number of exponential components observed in the open and closed dwell time distributions gives a lower estimate of the number of different states (i.e. protein conformations) associated with channel open and closed events respectively. It is also possible to predict theoretical probability distributions from the reaction rates using methods detailed by Colquhoun and Hawkes (1981). The theoretical predictions from the gating scheme are shown as solid curves in Figure 4B. Thus by fitting the data with these predictions it is possible to model the data in terms of rate constants between different conformational states of the channel.

A Study of Ca^{2+} and Mg^{2+} regulation of RyRs: An example of single channel analysis

The gating of RyRs depends on cytoplasmic Ca^{2+} and Mg^{2+} concentrations. RyRs from skeletal and cardiac muscle (ryr-1 and ryr-2 respectively) are activated by μM Ca^{2+} and inhibited by mM Ca^{2+} and Mg^{2+}. Several studies show that Mg^{2+} is a strong inhibitor of Ca^{2+} release in skeletal muscle (Owen *et al.*, 1997) and plays an important role in EC coupling (Lamb & Stephenson, 1991, Lamb & Stephenson, 1992). $^{45}Ca^{2+}$ release from skeletal SR vesicles suggests that regulation of RyRs by Mg^{2+} and Ca^{2+} is tied to two common mechanisms (Meissner *et al.*, 1986) but it was recognized that confirmation of that hypothesis awaited detailed single channel experiments. This section will show how single channel measurements of the Mg^{2+}- and Ca^{2+}-dependent gating kinetics in skeletal and cardiac RyRs identified two mechanisms for Mg^{2+}-inhibition. Details of this work can be found in (Laver *et al.*, 1997a, Laver *et al.*, 1997b, Laver *et al.*, 1995).

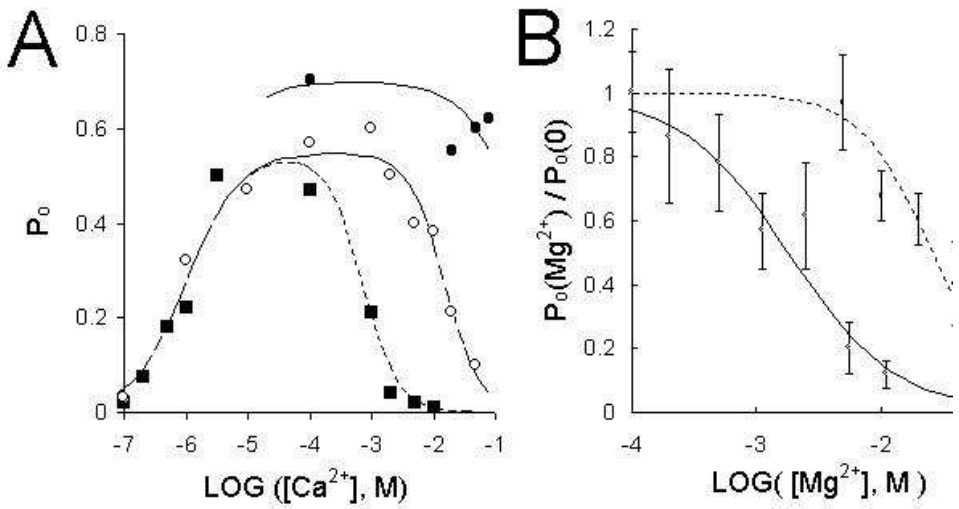

Figure 5. (*A) The dependence of the P_o on the cytoplsmic [Ca^{2+}] from three groups of RyR. (●)-sheep cardiac RyRs treated with CHAPS or high [CsCl] that were insensitive to inhibition by mM cis Ca^{2+}, (○)- native cardiac RyRs which could be inhibited by mM cis Ca^{2+}, (■)- rabbit skeletal RyRs. (B) The [Mg^{2+}]-dependence of the P_o of cardiac RyR in the presence of 1 mM Ca^{2+} (○) or 1 mM Ca^{2+} (●). The lines show Hill fits to the data (see below) using the following parameters: (solid line)- H = 1, K_m = 1.8 mM. (dashed line)- H = 1.5, K_m = 26 mM. The Hill equation used here relates the degree of channel inhibition by Mg^{2+} (P_o/P_ocontrol) to its binding affinity (K_m), Hill coefficient (H) and concentration:*

Analysis of the effects of non-physiological [Ca^{2+}] and [Mg^{2+}] can identify multiple mechanisms that are difficult to distinguish under physiological conditions.

It has long been recognized that there are two distinct Ca^{2+} regulation mechanisms in RyRs: one that activates them at μM cytoplasmic [Ca^{2+}] and another that inhibits them at mM [Ca^{2+}] (Meissner, 1994). This case study focuses on three groups of RyRs: Rabbit skeletal RyRs (■), sheep cardiac RyRs(○) and modified cardiac RyRs(●) which have been exposed to 500 mM CsCl or CHAPS detergent and so have lost their sensitivity to Ca^{2+} inhibition. An overall picture of the regulation of the three types of RyR by cytoplasmic Ca^{2+} is obtained from measurements of channel open probability (P_o) in Figure 5A. The three RyR types were similarly activated by cytoplasmic [Ca^{2+}] of ~ 1μM but they were differently inhibited by Ca^{2+}. Cardiac RyRs are, on average, 10 fold less sensitive to Ca^{2+} inhibition than skeletal RyRs, and cardiac RyR treated with CHAPS were not significantly inhibited by [Ca^{2+}], even at 100 mM. Mg^{2+} inhibited the three RyR groups. Once again, measurements of P_o give the overall picture of this inhibition. Increasing concentrations of Mg^{2+} progressively reduce the activity of RyRs (Figs. 5B and 6). Mg^{2+} differently inhibited the three RyR groups. Figure 7A shows the concentration of Mg^{2+} needed to reduce the P_o of RyRs by 50%, plotted against the Ca^{2+} concentration. The data in Figure 7 shows two broad features in the [Ca^{2+}] dependence of Mg^{2+} inhibition. One of these is an ascending limb where increasing [Ca^{2+}] causes the channel to become less sensitive to inhibition by Mg^{2+}. At low [Ca^{2+}] the Ca^{2+}-dependence of Mg^{2+} inhibition of the cardiac RyRs (both native and treated with CHAPS or CsCl) clearly show this ascending limb. There is also some indication of this with the skeletal RyRs at very low [Ca^{2+}]. The other feature is the plateau region, which occurs at higher [Ca^{2+}] where Mg^{2+} inhibition is insensitive to [Ca^{2+}]. This is clearly seen in the data from skeletal and cardiac RyRs in Figure 7A, although this was not apparent in the data obtained from RyRs treated with CHAPS or CsCl. A model for explaining the P_o data is shown schematically in Figure 8 in which there are two Ca^{2+} and Mg^{2+} dependent gates acting in series. One gate opens (activation gate) when the [Ca^{2+}] increases above 1 μM giving rise to Ca^{2+}-

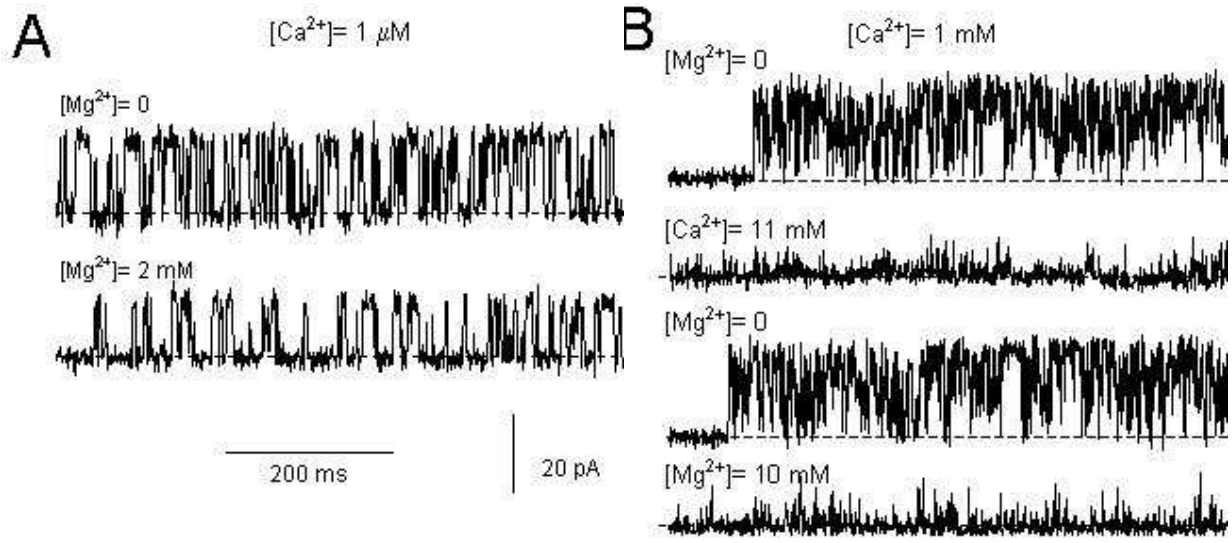

Figure 6. *Single channel recordings of sheep cardiac RyRs in lipid bilayers showing the effects of Mg^{2+}-inhibition on the pattern of channel gating. The cis bath contained 250 mM CsCl and the trans bath contained 50 mM CsCl. The potential difference across the bilayer is 40 mV (cis-trans) and the current baseline is at the bottom of each trace (dashed lines). (A) Mg^{2+}-inhibition in 1 mM Ca^{2+} appears to increase the duration of channel closures. (B) 10 mM Ca^{2+} was added to a RyR initially in 1 mM Ca^{2+} and this inhibits the channel. The cis bath was flushed with solutions containing 1mM Ca^{2+} and maximal channel activity was restored. Then 10 mM Mg^{2+} was added to the cis bath. Gating pattern of the RyR inhibited by 10 mM Mg^{2+} + 1 mM Ca^{2+} appeared to be the same as that inhibited by 11 mM Ca^{2+} alone. Mg^{2+}-inhibition in 1 mM Ca^{2+} also appeared to induce a more flickery gating pattern than in 1 mM Ca^{2+}.*

activation of the RyR. Another gate closes (inhibition gate) when [Ca^{2+}] rises to mM levels. Mg^{2+} at the activation gate reduces P_o by competing with Ca^{2+} for activation sites. However, Mg^{2+} is unable to open the channel. At the inhibition gate, Mg^{2+} and Ca^{2+} can each bind at the inhibition site and cause channel closure by a common mode of action. In this model the two gating mechanisms are assumed to operate concurrently and independently. The combined effect of both gates is such that the open probability of the channel is equal to the product of the open probabilities of each gate. It follows that the gating of the channel will tend to be dominated by the gate that is least open (see Fig. 7B) which explains why different inhibition mechanisms become apparent at low and high [Ca^{2+}].

Analysis of single channel gating kinetics can provide a stringent test for gating models.

If Ca^{2+} and Mg^{2+} do inhibit via a common mode of action then the kinetic signatures of Ca^{2+} and Mg^{2+} inhibition should be identical in the plateau region of the data (see Fig. 7). Moreover, the kinetic signature of Mg^{2+} inhibition in the plateau region should be different to that seen in the ascending limb since it is assumed that these two features arise from different mechanisms. Figure 9 shows that this is the case. Single channel recordings of native cardiac RyR inhibited by Mg^{2+} in the presence of low (1 μM) and high (1 mM) [Ca^{2+}] are shown in Figure 6 (different inhibition mechanism should be apparent at low and high [Ca^{2+}] see above). Inhibition by 2 mM Mg^{2+} in the presence of 1 μM Ca^{2+} reduced P_o to 50% of the control value and inhibition by10 mM Mg^{2+} in the presence of 1 mM Ca^{2+} also reduced P_o by 50%. Even though Mg^{2+} produced the same degree of inhibition in both cases, inspection of the pattern of gating in these records shows that Ca^{2+} and Mg^{2+} have very different effects on channel gating. Moreover, at high [Ca^{2+}], addition of either Ca^{2+} or Mg^{2+} produced

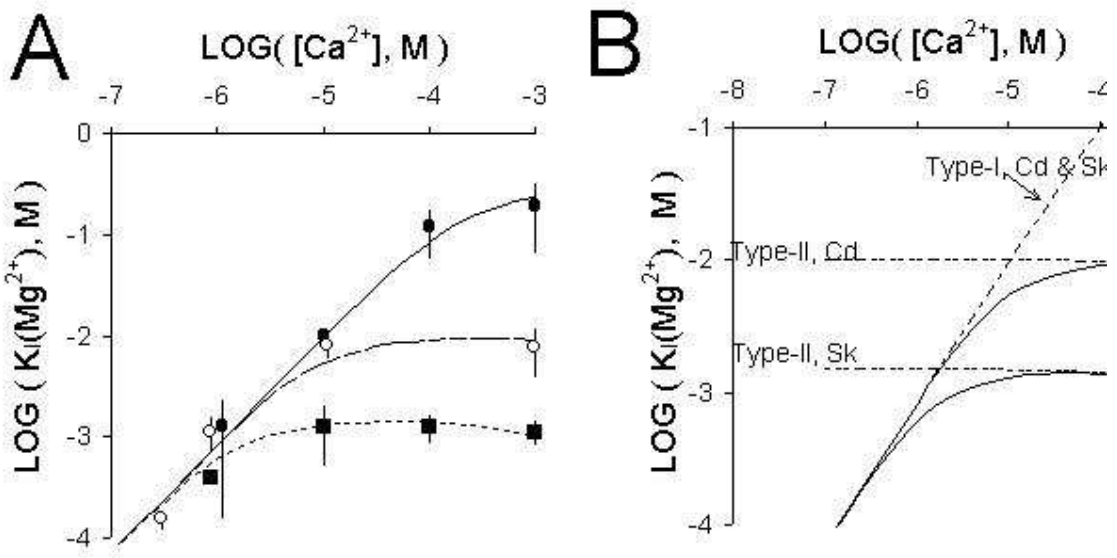

Figure 7 *(A) The mean (± sem) cis [Mg^{2+}] causing 50% inhibition of RyRs, $K_I(Mg^{2+})$, plotted against cis [Ca^{2+}] for three groups of RyR, namely, (●)-sheep cardiac RyRs treated with CHAPS or 500 mM [CsCl] that were insensitive to inhibition by mM cis Ca^{2+}, (○)- native cardiac RyRs which could be inhibited by mM cis Ca^{2+}. (■)- Rabbit skeletal RyRs. Three model predictions for the Ca^{2+}-dependence of $K_I(Mg^{2+})$, shown in part B, are compared with the data. (B) Model predictions for $K_I(Mg^{2+})$ showing the relative contributions of Mg^{2+}-inhibition at the activation and inhibition gates of cardiac (Cd) and skeletal (Sk) RyRs. The solid lines are two of the model fits to the data in Part A. The only difference between the two fits are due to differences in the affinity of Ca^{2+} and Mg^{2+} at the inhibition gate. The thick dashed lines show the Ca^{2+}-dependence of the [Mg^{2+}] required to halve the open probability of the activation and inhibition gates separately. It can be seen that for the cardiac RyRs (upper solid line) $K_I(Mg^{2+})$ at high and low [Ca^{2+}] extremes are similar to that expected solely from each inhibition mechanism separately.*

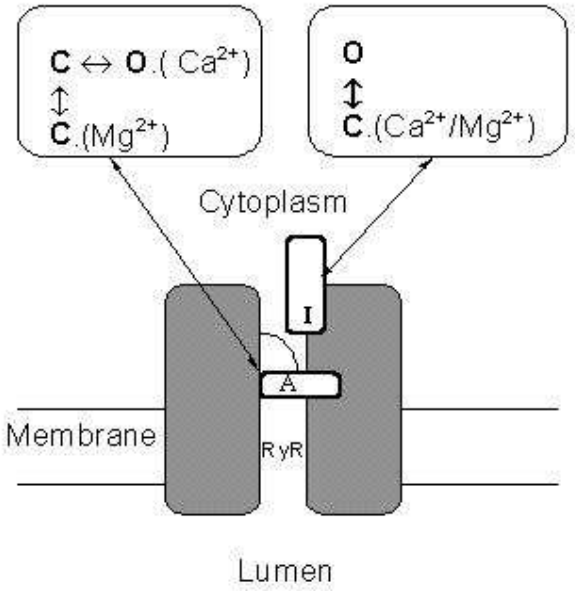

Figure 8. *A schematic diagram of a RyR which illustrates the main aspects of the model for Mg^{2+}-inhibition of RyRs. Gating mechanisms for Ca^{2+}-activation and Ca^{2+}-inhibition of the RyR are labelled (A) and (I) respectively. These gates are assumed to operate independently and such that both gates must be open for the channel to conduct. At the activation gate inhibition occurs when Mg^{2+} binds and prevents opening of the activation gate by competing with Ca^{2+} for the activation site. However, unlike Ca^{2+} binding (~1 mM affinity) the binding of Mg^{2+} at this site (~1 mM affinity) does not open the channel. At the inhibition gate, inhibition occurs with the binding of Mg^{2+} or Ca^{2+} (~ mM affinity) at a common set of sites.*

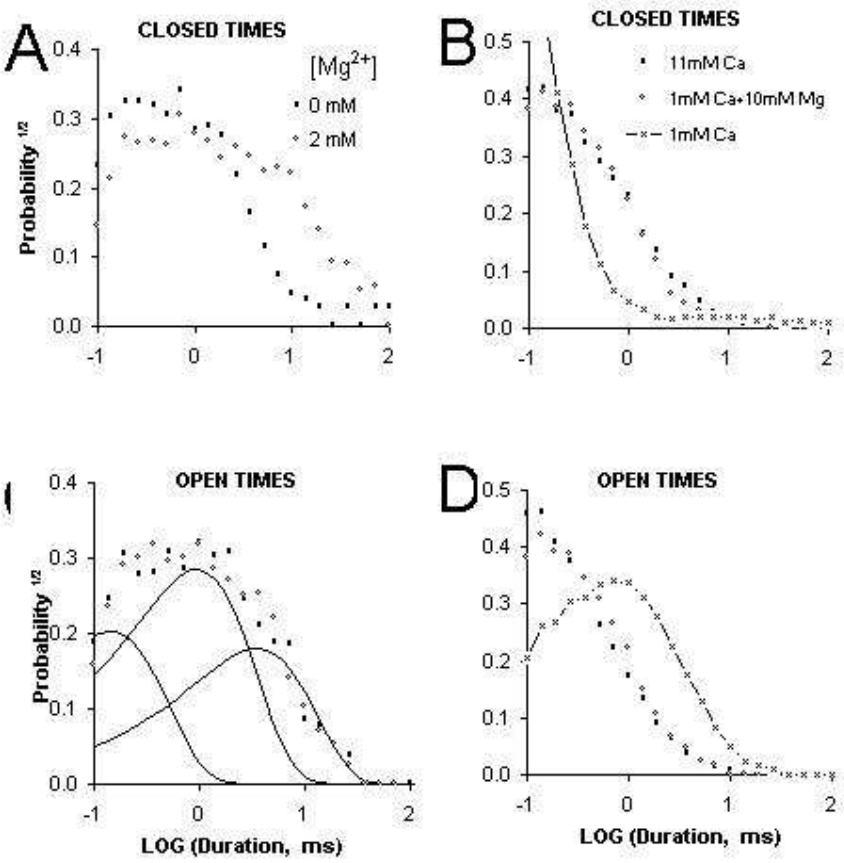

Figure 9. *Probability distributions of open and closed dwell times obtained from the same records as shown in Figure 6. (A&C) The effect of Mg^{2+} on the probability distributions closed (A) and open (C) dwell-times of cardiac RyRs in the presence of 1 mM cis [Ca^{2+}]. The probabilities were calculated from number of events/ bin divided by the total number of events (~1500 events in each record). The histograms were extracted from single channel recordings of ~15 second duration. The dwell-times are "log binned" and displayed using the approach of Sigworth and Sine (1987). The distributions of open and closed dwell-times could be fit by the sum of three exponentials shown separately by the three curves in part C. (B&D) The effect of Mg^{2+} on the probability distributions of channel closed (B) and open (D) dwell-times of cardiac RyRs in the presence of 1 mM [Ca^{2+}]. The gating of a single cardiac RyR was initially measured when the cis bath contained 1 mM $CaCl_2$ (æ xæ). The measurement was repeated after 10 mM $CaCl_2$ was added to the bath (open circles). The cis bath was then flushed with solution containing 1 mM $CaCl_2$. The cis [Mg^{2+}] was increased to 10 mM before the final measurement was made (closed circles). In both experiments a 50% inhibition of the RyR, by the addition of either 10mM Ca^{2+} or Mg^{2+}, had identical effects on channel gating.*

inhibition with a similar gating pattern. Probability histograms of open and closed dwell-times quantify these Mg^{2+}-inhibition effects on the channel gating. Inhibition by Mg^{2+} at low [Ca^{2+}] significantly increased the probability of long closed dwell-times (Fig. 9A) but produced no significant change in the open dwell-time distribution (Fig. 9C). In contrast, Mg^{2+} inhibition a high [Ca^{2+}] both increased the probability of long closed dwell-times (Fig. 9B) and increased the probability of short open dwell-times (Fig. 9D). Thus Mg^{2+} inhibition clearly has a different kinetic signature at high [Ca^{2+}] than at

low [Ca^{2+}]. However, the kinetic signatures of Ca^{2+} and Mg^{2+} inhibition at high [Ca^{2+}] are identical indicating that Ca^{2+} and
Mg^{2+} inhibit RyRs by modulating the same gating mechanism. It is highly unlikely that different mechanisms as complex as these (complex meaning that they are described by 6 exponentials and11 independent parameters) could, by coincidence, produce the same gating pattern.

Biophysical characterization of RyR regulation mechanisms has physiological relevance.

The fact that Ca^{2+} and Mg^{2+} share a common inhibitory mechanism provides an answer to the question of why RyRs are inhibited by mM cytoplasmic Ca^{2+} when [Ca^{2+}] never reach this level in muscle. Once it is realized that Mg^{2+} inhibition shares a common mechanism with Ca^{2+} and that Mg^{2+} is present at mM concentrations the answer becomes apparent. Thus it is likely that inhibition by Mg^{2+} is the physiologically relevant mechanism (as suggested by Lamb, 1993) and by focusing on Ca^{2+}-inhibition of RyRs one misses the physiologically important process. This interpretation sheds a new light on the molecular basis of Malignant Hyperthermia. Malignant hyperthermia (MH) is an inherited skeletal muscle disorder of humans and pigs that can be triggered in susceptible individuals by anesthetics, such as halothane, and by certain other agents and even by stress (Mickelson & Louis, 1996). The disorder is due to abnormal regulation of intracellular [Ca^{2+}] in the muscle cells due to over active RyRs. If an MH episode is initiated, it results in muscle rigidity, severe metabolic changes and excessive heat production, often leading to death if untreated. Porcine Malignant Hyperthermia is associated with the Arg615Cys mutation in the RyR, which alleviates RyR inhibition at mM [Ca^{2+}] (Mickelson & Louis, 1996). Because cytoplasmic [Ca^{2+}] never reaches mM levels it was not clear how the RyR mutation caused Malignant Hyperthermia. However, once it is realized that Ca^{2+} and Mg^{2+} share the same inhibitory mechanism then alleviation of Mg^{2+} inhibition becomes a plausible mechanism for altered Ca^{2+} release by RyRs. At physiological [Mg^{2+}] (~1 mM) RyRs from Malignant Hyperthermia susceptible muscle are less depressed by Mg^{2+} than normal RyRs. Therefore MH RyRs are more readily activated by any stimulus because cytoplasmic Mg^{2+} does not hold them as tightly shut as normal RyRs and this is a likely cause of the abnormally high Ca^{2+} release associated with this myopathy (Laver *et al.,* 1997b).

Variations between individual RyRs and different RyR types provide additional information about regulation mechanisms.

It is commonly found in single channel studies that the gating properties of ion channels differ to some extent from one channel to the next and RyRs are no exception to this. Several studies have focused on the heterogeneity of RyRs in bilayers (eg. Laver *et al.,* 1995, Copello *et al.,* 1997). While RyRs of one type all share common regulation mechanisms, there are substantial variations in RyR sensitivity to regulatory ligands such as ATP (Laver *et al.,* 2000b), Ca^{2+} (Laver *et al.,* 1995), Mg^{2+} (Laver *et al.,* 1997b, Laver *et al.,* 1997a) and pH (Laver *et al.,* 2000a). This variability provides an opportunity to examine correlations between different properties of the RyR that would suggest common underlying mechanisms. For example, if Ca^{2+} and Mg^{2+} do inhibit RyRs by a common mechanism then their sensitivity to Ca^{2+} should be correlated with their sensitivity to Mg^{2+}. The Mg^{2+} sensitivity of cardiac RyRs varied by an order of magnitude between individual channels. Half inhibition by Mg^{2+} in the presence of high [Ca^{2+}] (in the plateau region, see Fig. 7) occurred at [Mg^{2+}] ranging from 2 to 10 mM. The sensitivity to Ca^{2+} and Mg^{2+} inhibition in the variable RyR population were compared in the same RyR as shown in Figure 10, which shows a good correlation and equality between half inhibiting concentrations of Ca^{2+} and Mg^{2+}. In addition to variations between individual RyRs of one group there are systematic differences in the mean sensitivity of different groups of RyRs to Ca^{2+} and Mg^{2+} inhibition. In this regard, cardiac RyRs are less sensitive than skeletal RyR and skeletal RyRs with the MH mutation are less sensitive than normal skeletal RyRs. When the sensitivity

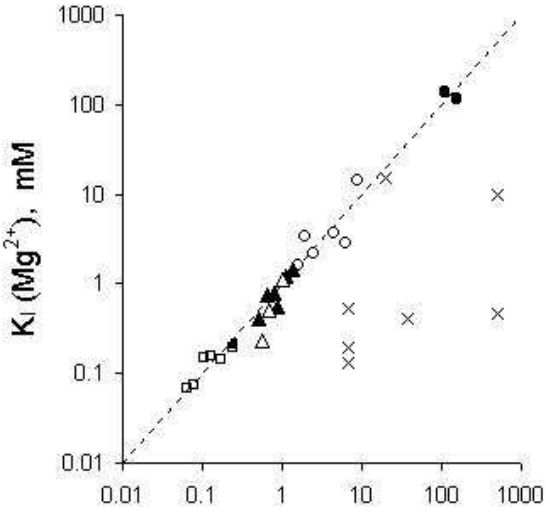

Figure 10. *Correlation between the sensitivity to inhibition by Ca^{2+} and Mg^{2+} in individual RyRs. Half inhibition by Mg^{2+}, $K_I(Mg^{2+})$, and by Ca^{2+}, $K_I(Ca^{2+})$, was determined on the same RyRs. The correlation between $K_I(Mg^{2+})$ and $K_I(Ca^{2+})$ is also shown for different groups of RyR which have, on average, different sensitivities to Ca^{2+} and Mg^{2+} inhibition. Within each group there is significant variation in these properties. Unless otherwise stated cis $[Cs^+]$=250 mM; (○)- cardiac RyRs in the presence of 1mM Ca^{2+} where they showed normal Ca^{2+}-inhibition, (●)-cardiac RyRs in the presence of 1mM Ca^{2+} where they showed reduced Ca^{2+}-inhibition because they had been exposed to cis 500 mM CsCl or CHAPS for one minute prior to measurements of divalent ion inhibition, (□)- normal pig skeletal RyRs in the presence of 50 mM Ca^{2+} and 100 mM CsCl (■)-MHS RyRs in the presence of 50 mM Ca^{2+} and 100 mM CsCl. (△)-normal pig skeletal RyRs in the presence of 50 mM Ca^{2+}, (▲)-MHS pig skeletal RyRs in the presence of 50 mM Ca^{2+}. (X)- cardiac RyR in the presence of less than 100 mM Ca^{2+}.*

of individual RyRs to Ca^{2+} and Mg^{2+} inhibition are compared across a range of RyR types there is a tight correlation and equality between the half inhibiting concentrations of Ca^{2+} and Mg^{2+} over three orders of magnitude (correlation coefficient, r = 0.96 or coefficient of determination, r^2=0.9). In contrast to this was the lack of any correlation (r = 0.17) between Ca^{2+} and Mg^{2+} inhibition when Mg^{2+} inhibition was measured in the presence of low $[Ca^{2+}]$. This clearly shows that the Mg^{2+}/Ca^{2+} equivalence does not apply under low $[Ca^{2+}]$ conditions suggesting that Mg^{2+} inhibition at low $[Ca^{2+}]$ are due to a different mechanism to Ca^{2+} inhibition.

Functional interactions between RyRs and other endogenous proteins.

Several proteins are now known to have effects on the activity of the RyR in muscle. The most notable of these is the DHPR (see above). In addition there is also calmodulin, calsequestrin, triadin, junctin and the FK506 binding protein (FKBP). These proteins are believed to form part of a large complex that is the machinery for EC coupling in muscle. With bilayer methods it has been possible to dismantle the EC-coupling machine to gain clues as to how the individual components contribute to its overall function. With the likely exception of the DHPR, native RyRs in lipid bilayers appear to remain associated with the above-mentioned co-proteins. The effects of these co-proteins on RyR activity have been studied in lipid bilayers by dissociating these proteins while simultaneously recording channel activity. Biochemical methods such as SDS-PAGE, Western blots and radio active labeling have been used to confirm that the treatments used to dissociate RyR co-proteins in lipid bilayer experiments are specific to the protein of interest. This approach has been used to study interactions between RyRs and calmodulin (Tripathy *et al.*, 1995), calsequestrin (Beard *et al.*, 2000, Beard *et al.*, 1999) and FKBP (Ahern *et al.*, 1997). So far this approach has not proved successful for studying the effect of DHPRs on RyRs in lipid bilayers. However, inroads into this area have been made using less direct means. The DHPR and RyR in skeletal muscle are believed to interact via the cytoplasmic loop region between transmembrane repeats II and III of the DHPR α_1 subunit (aa 666-791, Tanabe *et al.*, 1990). The isolated skeletal II-III loop has been added to single RyRs in bilayers and was found to activate them (Lu *et al.*, 1994). Also, synthetic peptides, encompassing regions of the skeletal II-III loop have been applied to RyRs and were found to regulate RyR activity (Dulhunty *et al.*, 1999).

An example of how single channel experiments have been used to study the functional interactions between RyRs and other proteins is the investigation of calsequestrin. Calsequestrin is a protein found in the lumen of the SR, which acts as a moderate affinity (K_D=1 x 10^{-5} M) Ca^{2+} binding protein that buffers the luminal free [Ca^{2+}] (MacLennan & Wong, 1971). Two other proteins, triadin and junctin, span the SR membrane and these proteins bind to both calsequestrin and the RyR (Knudson *et al.,* 1993, Kanno & Takishima, 1990, Zhang *et al.,* 1997, Jones *et al.,* 1995, Guo *et al.,* 1996). SDS-PAGE and Western Blotting techniques have shown that calsequestrin can be dissociated from the RyR complex by exposing SR membranes to raised ionic strength (ie 500 mM as apposed to 250 mM), or by exposing them to higher than usual [Ca^{2+}] (13 mM as apposed to 1 mM). By applying similar solutions changes to RyRs in bilayers it was possible to see the effects of a calsequestrin dissociation event during recordings of RyR activity. To do this the ionic strength or [Ca^{2+}] of the luminal bath in bilayer experiments was increased like that in the SDS-PAGE experiments. This caused an increase in RyR activity that could only be reversed by addition of purified calsequestrin to the luminal bath. The presence or absence of calsquestrin on the RyR in bilayers was confirmed using an anti-calsequestrin antibody that inhibits channel activity when it binds to the calsequestrin-RyR complex. The data were consistent with an overall picture in which calsequestrin dissociation enhanced native RyR activity and calsequestrin binding suppressed channel opening. The next step would be to assess the combined effects of triadin, junctin and calsequestrin on RyR activity. Junctin and triadin can be dissociated from the RyR by solublising the SR membranes with CHAPS detergent and purifying the RyR. Thus by applying triadin, junctin and calsequestrin, in various combinations, to purified RyRs in bilayer experiments it will be possible to systematically piece together these components of the EC coupling machinery and measure their effects on RyR activity.

RyR function and its relationship to its tetrameric structure

Electron microscope image reconstruction shows RyRs to have four-fold symmetry (Orlova *et al.,* 1996). This four-fold symmetry means that each of the four subunits must somehow contribute equally to ligand binding and channel gating. Therefore the mechanisms regulating channel gating are likely to be complex. Single channel studies are now starting to give an insight into how homotetrameric structures like the RyR control channel activity.

Four-fold structure inferred from channel conductance.

Telltale signs of the contribution of four subunits to channel conductance appeared not long after the discovery of the RyR (Ma *et al.,* 1988, Smith *et al.,* 1988). RyRs displayed multiple conductance levels with subconductances near 25%, 50% and 75% of the maximum (ie equally spaced levels) conductance level. These were interpreted a current flow through pores formed by the activation of different numbers of subunits; 25% corresponding to one, 50% to two subunits etc. Very clear and sustained substate activity at approximately equally spaced levels has been observed in RyRs that were modified either by the binding of ryanodine (Ma & Zhao, 1994) or the stripping of the FKBP, a co protein to the RyR (Ahern *et al.,* 1997). Amplitude histograms of channel activity revealed that the spacing of substates was not exactly equal. Nonetheless, these studies interpreted the substates as the opening of four separate conducting pathways in the channel. These must gate cooperatively and simultaneously in order to produce the observed gating of the RyR complex between closed and maximum conductance levels in a single transition. More recently mutations in the RyR have been discovered that alter channel conductance and experiments with hybrid RyRs containing these mutations have shed more light on subunit contributions to channel conductance. A highly conserved 10 amino acid segment within the pore-forming region about aa4824 was found to be the determinant of channel conductance (Zhao *et al.,* 1999). Single channel studies showed that the glycine to alanine substitution, G4824A, reduced channel conductance by 97%. Co-expression of mutant and wild-type

subunits produced a range of hybrid channel types with six different maximal conductance levels that lie between those of the homozygous mutant and wild-type RyRs. The number of different conductance levels corresponds to the number of subunit combinations that are possible with two types of subunits in a tetramer. The fact that six conductance levels could be observed suggest that the four subunits somehow contribute to a single conduction pathway through the RyR as apposed to the idea that each subunit possesses a separate pathway.

Four-fold structure inferred from steady state channel gating.

The gating of RyRs has exhibited phenomena that suggest mechanisms stemming from a tetrameric structure. The Arg615Cys mutation (MH mutation in pigs, see above) in the RyR alleviates RyR inhibition at mM [Ca^{2+}] and [Mg^{2+}]. Shomer *et al.* (1995) found that RyRs expressed in heterozygous pigs gave rise to hybrid RyRs with gating properties intermediate to those of the wild type and mutant. This indicated that each subunit in the RyR tetramer has an influence over the Ca^{2+} sensitivity of the channel. More recently, Chen *et al.* (1998) discovered an alanine to glutamate substitution, E3885A, which decreased the sensitivity of RyR to Ca^{2+} activation by four orders of magnitude such that mM levels of cytoplasmic Ca^{2+} were required to activate the channel. Co-expression of subunits containing altered sites for Ca^{2+}-activation with wild-type subunits produced five or six types of RyRs with sensitivities to Ca^{2+} activation ranging between those seen for the mutant and wild type homotetramers. Chen *et al.* (1998) suggested that all four subunits contribute to each Ca^{2+} activation site. A more detailed interpretation of these experiments awaits the development of methods for linking the stoichiometry of the hybrid channels with the observed channel function.

Four-fold structure inferred from non-steady state channel gating.

Aspects of the tetrametric structure of RyRs may also show up in the response of RyRs to rapid changes in the concentration of regulatory ligands. It is recognized that during muscle contraction the RyRs respond to rapid (~ms) step increases in [Ca^{2+}] resulting from Ca^{2+} flow through nearby dihydropyridine and ryanodine receptors. Consequently there has been considerable interest in the effects of rapid [Ca^{2+}] transients on the activity of RyRs in bilayers (see perspectives by Sitsapesan & Williams, 2000, Lamb *et al.*, 2000, Fill *et al.*, 2000). Now there is also a growing interest in the effects of rapid application of other regulatory ligands such a protons (Laver *et al.*, 2000a). The effect of steady cytoplasmic pH on RyRs has been addressed in several studies (Rousseau & Pinkos, 1990, Shomer *et al.*, 1994, Ma *et al.*, 1988), which show acid pH inhibits RyRs; with half inhibition at pH6.5 and with near total inhibition below pH6. However, rapid changes in pH reveal new characteristics of RyR gating not apparent in steady state recordings. The pH was increased from ~5.5 (inhibiting pH) to above 7 (activating pH) over a 500 ms period by squirting solutions from a perfusion tube placed in the vicinity of the bilayer. Rather than activating in a graded manner reflecting the continuous change of pH over this period, the RyRs activate in a stepwise manner. As the RyRs activate their open probability RyRs increases in what appears to be different gating modes with ascending P_o (see Fig. 11A). Amplitude histograms of RyR P_o (Fig. 11B) show four of these gating modes as four distinct peaks. The four gating modes correspond in number to what would be expected if RyR subunits activated separately in response to proton dissociation. Thus the first, lowest P_o mode would be when one subunit is active and higher P_o modes would occur as more of the four subunits activated. If this hypothesis were correct then the stability of ligand mediated channel openings would depend on the number of subunits that have bound ligand molecules. This phenomenon has been seen in the cyclic nucleotide gated channel (Ruiz & Karpen, 1997).

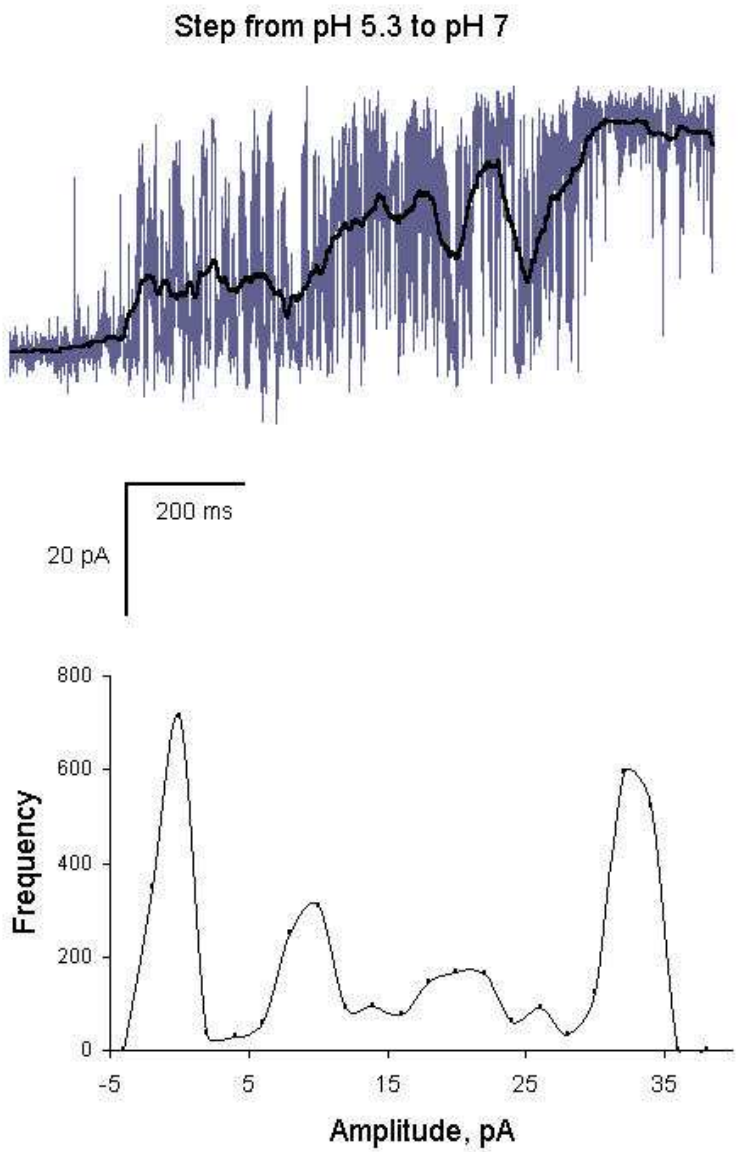

Figure 11. (*A) Recording of a single RyR showing recovery from inhibition at low pH. The cytoplasmic pH was rapidly raised (~1s) from 5.3 to 7 by moving a solution stream from a tube onto and away from the bilayer. The onset of solution change occurred at the beginning of the trace. In the first 200 ms the channel showed slight activation (P_o~0.01) that jumped to a P_o of 0.3 at 200ms, 0.6 at 400 ms and 1.0 at 800 ms into the record. The heavy line shows a running average of the current record, which rises in a stepwise manner as the channel activates. (B) The amplitude histogram of the running average showing peaks, which correspond to relatively stationary segments of activity in part A. The weakest activation seen in the first 200 ms produced the peak at zero current and the other three modes of activity give rise to peaks at 6pA, 20pA and 34 pA.*

Future directions in single channel recording

The rate at which single channel recording techniques have advanced our knowledge is generally limited by the rate at which good recordings can be obtained from either membrane patches or artificial bilayers. Single channel recording is a slow and tedious process where progress is constrained by a range of technical limitations. First, the techniques are notoriously hit and miss in that they do not provide control over the number and types of channels observed. It is common for

experiments to be confounded by the appearance of more than a single channel, the appearance of the wrong channel type or the non-appearance of any channel. Secondly, these membrane systems are extremely fragile and rupture of membrane patches and bilayers terminate experiments within minutes. This severely restricts the range of experimental protocols that can be used for single channel recordings. Any way of overcoming these problems would provide a major advance in single channel recording techniques. This section describes a number of new methods for producing robust, long-lived membrane systems that could be applied to studying individual ion channels.

As described above, the most commonly used method of making planar bilayers is the film drainage method, which was developed by (Mueller *et al.,* 1962). Tien, one of the authors on the original bilayer paper, has published several new methods for forming robust lipid bilayers using solid supports (Ottova & Tien, 1997). As before, bilayers are formed from solutions of lipids in hydrophobic solvents such as n-decane. However, instead of producing lipid films that are suspended across an aperture, bilayer membranes are formed from lipid films spread across solid or gel surfaces. The viscous support offered by a nearby solid surface boosts enormously the stability of the bilayer. Doping these stable membranes with various substances has been shown to endow these membranes with a range of useful properties such as ion selectivity (by incorporation of ionophors such as gramicidin), immunologic reactivity (with antibodies), electron transporters (with C_{60} fullerenes) and photosensitivity (with Zn-phthalocyanine) (Ottova & Tien, 1997, Tien *et al.*, 1991). However, the advantages of supported bilayer systems have not yet been realised in single channel studies. If one could incorporate RyRs, for example, into bilayers on agar supports then conventional electrophysiology experiments could be carried out on a single channel over extended periods of time (hours). Moreover, because the supported bilayers are robust and usually made on the end of electrodes, they are remarkably manoeuvrable. Hence, these bilayers could be aligned within complex measuring apparatus such as those using confocal microscopy or rapid perfusion. The rate and quality of data acquired this way would be far superior to that obtained using conventional bilayer methods.

More recently solid substrate bilayer methods were further improved by developing bilayer structures that could be chemically anchored to a gold surface (Cornell *et al.,* 1997). These were developed for the purpose of making a new generation of biosensors. These systems are remarkably robust: being able to be stored dehydrated for periods of many months. In principle, ion channels could be embedded in these membranes though no successful attempts to do this have been published. Future developments of this system could revolutionise bilayer-based methods of single channel recording. In the future one might purchase bilayers off the shelf and perform weeks of experiments on a single ion channel. Moreover, the hit and miss aspect of single channel methods (see above) may soon be a thing of the past. It is recognised in the biosensor industry that biosensors based on arrays of detectors can offer vastly superior combination of detection sensitivity and speed. Once these bilayer array platforms are produced then the scope for single channel recording is truly enormous. Incorporation of ion channels onto arrays of 10,000 or more electrically isolated bilayers will allow an experimenter to select bilayers in the array that contain the desired number and type of ion channels. One could easily work with mixtures of ion channels as found, for example, in SR membranes because one could choose particular bilayers that contained only the ion channels of interest. It will also be possible to get information from individual ion channels at the same time as obtaining measurements of the average response of many channels by averaging signals from many bilayers. In fact, a highly parallel solid-state electrode array has been developed for patch-clamping that makes possible multiple, simultaneous, single-cell electrical recordings (Axon instruments press release). Thus by layering cells onto these arrays one can simultaneously obtain single-channel and whole-cell currents. So it appears that even now the former limits to data acquisition are giving way to new frontiers in which the rate-limiting factor will be the rate at which data can be acquired with massively parallel detection systems.

Concluding remarks

The regulation of RyR channels by intracellular metabolites such as ATP, Ca^{2+}, Mg^{2+} and pH is a complex interplay of several regulation processes. Overlayed on this is the fact that these mechanisms are modulated by oxidation and phosphorylation mediated modifications of the RyR and by RyR interactions with a variety of co-proteins. Consequently, in order to understand how RyRs are regulated by normal metabolism or during muscle fatigue and myocardial ischemia it is necessary to deal with the very complex problem of understanding RyR function. Single channel recording and analysis methods are powerful enough to examine RyRs in sufficient detail to dissect the complex regulation mechanisms operating in RyRs. The enormous scope with the bilayer method for manipulating the quaternary structure of the EC-coupling machinery have allowed us to probe the effects of DHPRs, calmodulin, calsequestrin, triadin and the FKBP on RyR function. Three examples of forays into these areas by single channel studies have been described here. First, the analysis of [Ca^{2+}] and [Mg^{2+}] regulation of RyRs showed how it is possible to identify and characterise multiple mechanisms by which a single ligand can regulate RyRs and how this leads to an improved understudying of physiological processes in muscle. Secondly, experiments with RyRs in which co-proteins such as calsequestrin and triadin were systematically removed and replaced show how it is possible to understand the functional importance interactions between RyRs and co-proteins. Finally, investigations of the relationship between structure and function of native and mutated RyRs showed several aspects of RyR that reflects the four-fold symmetry of the RyRs structure. However, this area is still at an early stage and it is not yet clear how the four identical subunits of the RyR cooperate in regulating RyR gating.

In spite of the power of single channel recording the bilayer method has an Achilles heel. The fact that RyRs are studied in isolation means that it is not possible to examine their function in the physiological context. Hence one cannot directly apply RyR phenomena in bilayers to the physiological situation. However, the underlying mechanisms for RyR regulation identified from bilayer measurements are likely to apply to the *in vivo* situation and so contribute to our understanding of EC-coupling. On the other hand, studies of more intact muscle preparations such as suspensions of SR vesicles and mechanically skinned fibres are well suited for addressing the physiological situation. However, these systems are complex and it is difficult to identifying underlying mechanisms from the experimental data. Parallel experiments on lipid bilayers and muscle preparations in which the machinery for EC coupling is still intact have proved to be a powerful tool for elucidating mechanisms of Ca^{2+} regulation in muscle. In this collaboration of techniques the bilayer studies identify the basic mechanisms of channel function and the experiments on intact systems show the outworking of these mechanisms in the physiological situation.

Acknowledgements

We wish to thank Dr. Graham Lamb for his helpful comments. This work was supported by the National Health & Medical Research Council of Australia (Grant #9936486).

References

Ahern, G.P., Junankar, P.R. & Dulhunty, A.F. (1997) Subconductance states in single channel activity of skeletal muscle ryanodine receptors after removal of FKBP12. *Biophysical Journal,* 72, 146-162.

Ashley, C.C., Mulligan, I.P. & Lea, T.J. (1991) Ca^{2+} and activation mechanisms in skeletal muscle *Quarterly Reviews in Biophysics,* 24, 1-73.

Beard, N.A., Dulhunty, A.F. & Laver, D.R. (2000) The effect of increasing luminal calcium on skeletal muscle *Proceedings of the Australian Physiological and Pharmacological Society,* 31, 22P.

Beard, N.A., Laver, D.R. & Dulhunty, A.F. (1999) Regulation of skeletal muscle ryanodine receptors by calsequestrin *Proceedings of the Australian Physiological and Pharmacological Society*, 30, 43P.

Chen, S.R., Ebisawa, K., Li, X. & Zhang, L. (1998) Molecular identification of the ryanodine receptor Ca^{2+} sensor. *Journal of Biological Chemistry*, 273, 14675-14678.

Colquhoun, D. & Hawkes, A.G. (1981) On the stochastic properties of single ion channels *Proceedings Royal Society London Biol*, 211, 205-235.

Copello, J.A., Barg, S., Onoue, H. & Fleischer, S. (1997) . Heterogeneity of Ca^{2+} gating of skeletal muscle and cardiac ryanodine receptors. *Biophysical Journal*, 73, 141-156.

Cornell, B.A., Braach-Maksvytis, V.L., King, L.G., Osman, P.D., Raguse, B., Wieczorek, L. & Pace, R.J. (1997) A biosensor that uses ion-channel switches. *Nature*, 387, 580-583.

Dulhunty, A.F., Laver, D.R., Gallant, E.M., Casarotto, M.G., Pace, S.M. & Curtis, S. (1999) Activation and inhibition of skeletal RyR channels by a part of the skeletal DHPR II-III loop: effects of DHPR Ser687 and FKBP12 *Biophysical Journal*, 77, 189-203.

Fill, M., Zahradnikova, A., Villalba-Galea, C.A., Zahradnik, I., Escobar, A.L. & Gyorke, S. (2000) . Ryanodine receptor adaptation. *Journal of General Physiology*, 116, 873-82.

Guo, W., Jorgensen, A.O. & Campbell, K.P. (1996) Triadin, a linker for calsequestrin and the ryanodine receptor. *Society of General Physiologists Series*, 51, 19-28.

Jones, L. R., Zhang, L., Sanborn, K., Jorgensen, A.O. & Kelley, J. (1995) Purification, primary structure, and immunological characterization of the 26-kDa calsequestrin binding protein (junctin) from cardiac junctional sarcoplasmic reticulum. *Journal of Biological Chemistry*, 270, 30787-96.

Kanno, T. & Takishima, T. (1990) Chloride and potassium channels in U937 human monocytes. *Journal of Membrane Biology*, 116, 149-161.

Knudson, C. M., Stang, K. K., Jorgensen, A. O. & Campbell, K. P. Biochemical characterization and ultrastructural localization of a major junctional sarcoplasmic reticulum glycoprotein (Triadin). *Journal of Biological Chemistry*, (1993) 268, 12637-12645.

Lamb, G.D. (1993) Ca^{2+} inactivation, Mg^{2+} inhibition and malignant hyperthermia [news]. *Journal of Muscle Research and Cell Motility*, 14, 554-556.

Lamb, G.D., Laver, D. R. & Stephenson, D.G. (2000) Questions about Adaptation in Ryanodine Receptors. *Journal of General Physiology*, 116, 883-890.

Lamb, G.D. & Stephenson, D.G. (1991) Effect of Mg^{2+} on the control of Ca^{2+} release in skeletal muscle fibres of the toad. *Journal of Physiology*, 434, 507-528.

Lamb, G.D. & Stephenson, D.G. (1992) Importance of Mg^{2+} in excitation-contraction coupling in skeletal muscle. *News in Physiological Sciences*, 7, 270-274.

Laver, D.R., Baynes, T.M. & Dulhunty, A.F. (1997a) *Journal of Membrane Biology*, 156, 213-229.

Laver, D.R., Eager, K.R., Taoube, L. & Lamb, G.D. (2000a) *Biophysical Journal*, 78, 1835-1851.

Laver, D.R., Lenz, G.K.E. & Lamb, G.D. (2000b) *Proceedings of the Australian Physiological and Pharmacological Society*, 31, 7P.

Laver, D.R., Owen, V.J., Junankar, P.R., Taske, N.L., Dulhunty, A.F. & Lamb, G.D. (1997b) Reduced inhibitory effect of Mg^{2+} on ryanodine receptor-Ca^{2+} release channels in malignant hyperthermia. *Biophysical Journal*, 73, 1913-1924.

Laver, D.R., Roden, L.D., Ahern, G.P., Eager, K.R., Junankar, P.R. & Dulhunty, A.F. (1995) Cytoplasmic Ca^{2+} inhibits the ryanodine receptor from cardiac muscle. *Journal of Membrane Biology,* 147, 7-22.

Lu, X., Xu, L. & Meissner, G. (1994) Activation of the skeletal muscle calcium release channel by a cytoplasmic loop of the dihydropyridine receptor. *Journal of Biological Chemistry,* 269, 6511-6.

Ma, J., Fill, M., Knudson, C. M., Campbell, K. P. & Coronado, R. (1988) Ryanodine receptor of skeletal muscle is a gap junction-type channel. *Science,* 242, 99-102.

Ma, J. & Zhao, J. (1994) . Highly cooperative and hysteretic response of the skeletal muscle ryanodine receptor to changes in proton concentrations. *Biophysical Journal,* 67, 626-633.

MacLennan, D. H. & Wong, P. T. (1971) Isolation of a calcium-sequestering protein from sarcoplasmic reticulum. *Proceedings of the National Academy of Sciences USA,* 68, 1231-1235.

Meissner, G. (1994) Ryanodine receptor/Ca^{2+} release channels and their regulation by endogenous effectors. *Annual Review of Physiology,* 56, 485-508.

Meissner, G., Darling, E. & Eveleth, J. (1986) Kinetics of rapid Ca^{2+} release by sarcoplasmic reticulum. Effects of Ca^{2+}, Mg^{2+}, and adenine nucleotides. *Biochemistry,* 25, 236-244.

Mickelson, J. R. & Louis, C. F. (1996) Malignant hyperthermia: Excitation-contraction coupling, Ca^{2+} release channel, and cell Ca^{2+} regulation defects. *Physiological Reviews,* 76, 537-592.

Miller, C. & Racker, E. (1976) Ca^{++}-induced fusion of fragmented sarcoplasmic reticulum with artificial planar bilayers. *Cell,* 9, 283-300.

Mueller, P., Rudin, D. O., Tien, H. T. & Westcott, W. C. (1962) . Reconstitution of cell membrane structure in vitro and its transformation into an excitable system. *Nature,* 194, 979-981.

Nabauer, M., Callewaert, G., Cleemann, L. & Morad, M. (1989) Regulation of calcium release is gated by calcium current, not gating charge, in cardiac myocytes. *Science,* 244, 800-803.

Neher, E. & Sakmann, B. (1976) Single-channel currents recorded from membrane of denervated frog muscle fibres. *Nature,* 260, 799-802.

Ogawa, Y. (1994) Role of ryanodine receptors. *Critical Reviews of Biochemistry and Molecular Biology,* 29, 229-74.

Orlova, E. V., Serysheva, I. I., Van Heel, M., Hamilton, S. L. & Chiu, W. (1996) Two structural configurations of the skeletal muscle calcium release channel. *Nature Structural Biology,* 3, 547-552.

Ottova, A. L. & Tien, H. T. (1997) Self-assembled bilayer lipid membranes: from mimicking biomembranes to practical applications. *Bioelectrochemistry and Bioenergetics,* 42, 141-152.

Owen, V. J., Taske, N. L. & Lamb, G. D. (1997) Reduced inhibitory effect of Mg^{2+} on Ca^{2+} release in porcine muscle fibers with ryanopdine receptor mutation for malignant hyperthermia *American Journal of Physiology,* 272, C203-211.

Rousseau, E. & Pinkos, J. (1990) pH modulates conducting and gating behaviour of single calcium release channels. *Pflugers Archiv,* 415, 645-647.

Ruiz, M. L. & Karpen, J. W. (1997) Single cyclic nucleotide-gated channels locked in different ligand- bound states. *Nature,* 389, 389-392.

Shomer, N. H., Mickelson, J. R. & Louis, C. F. (1994) Caffeine stimulation of malignant hyperthermia-susceptible sarcoplasmic reticulum Ca^{2+} release channel. *American Journal of Physiology,* 267, C1253-C1261.

Shomer, N. H., Mickelson, J. R. & Louis, C. F. (1995) Ca^{2+} release channels of pigs heterozygous for malignant hyperthermia. *Muscle Nerve,* 18, 1167-1176.

Sigworth, F. J. & Sine, S. M. (1987) Data transformations for improved display and fitting of single- channel dwell time histograms. *Biophysical Journal,* 52, 1047-1054.

Sitsapesan, R. & Williams, A. J. (2000) Do inactivation mechanisms rather than adaptation hold the key to understanding ryanodine receptor channel gating?*Journal of General Physiology*, 116, 867-72.

Smith, J. S., Imagawa, T., Ma, J., Fill, M., Campbell, K. P. & Coronado, R. (1988) Purified ryanodine receptor from rabbit skeletal muscle is the calcium-release channel of sarcoplasmic reticulum. *Journal of General Physiology*, 92, 1-26.

Tanabe, T., Beam, K. G., Adams, B. A., Niidome, T. & Numa, S. (1990) . Regions of the skeletal muscle dihydropyridine receptor critical for excitation-contraction coupling. *Nature*, 346, 567-569.

Tien, H. T., Salamon, Z. & Ottova, A. (1991) . Lipid bilayer-based sensors and biomolecular electronics. *CriticalReviews in Biomedical Engineering*, 18, 323-340.

Tripathy, A., Xu, L., Mann, G. & Meissner, G. (1995) Calmodulin activation and inhibition of skeletal muscle Ca^{2+} release channel (ryanodine receptor). *Biophysical Journal*, 69, 106-119.

Zhang, L., Kelley, J., Schmeisser, G., Kobayashi, Y. M. & Jones, L. R. (1997) . Complex formation between junctin, triadin, calsequestrin, and the ryanodine receptor. Proteins of the cardiac junctional sarcoplasmic reticulum membrane. *Journal of Biological Chemistry*, 272, 23389-23397.

Zhao, M., Li, P., Li, X., Zhang, L., Winkfein, R. J. & Chen, S. R. (1999) . Molecular identification of the ryanodine receptor pore-forming segment. *Journal of Biological Chemistry*, 274, 25971-25974.